Comparative Study of Roman Iron Slags Discovered in the Roman Auxiliary Fort and Settlement of Călugăreni

Enikő BITAY[1], Irén KACSÓ[2], Szilamér Péter PÁNCZÉL[3], Erzsébet VERESS[4]

[1] *Sapientia Hungarian University of Transylvania, Faculty of Technical and Human Sciences, Târgu-Mureş, Romania, ebitay@ms.sapientia.ro*

[2] *National Institute for Research and Development of Isotopic and Molecular Technologies (INCDTIM), Cluj-Napoca, Romania, iren.kacso@gmail.com*

[3] *Mureş County Museum, Târgu-Mureş, Romania, pszilamer@yahoo.com*

[4] *Transylvanian Museum Society, Cluj-Napoca, Romania, veresserzsebet@gmail.com*

Abstract

Iron slag samples unearthed at the eastern border of Roman Dacia, in the auxiliary fort and the military settlement of Călugăreni (Mikháza) are investigated by macroscopic inspection, optical microscopy (OM) and FTIR spectroscopy in order to comparatively characterize their macro- and microstructure as well as their mineralogical composition. During the recent archaeological excavations, a large number of iron artefacts were discovered together with a great quantity of iron slag fragments. The present paper focuses on the data obtained from 17 slag samples.

Keywords: *iron slags, macroscopic investigation, optical microscopy, FTIR spectroscopy.*

1. Introduction

Among other resources, the procurement of rich ore and salt mines were a determining factor in the decision of the Romans to conquer Dacia. In the territory of the defeated Dacian kingdom a Roman province was organized at the beginning of the 2nd century, and continued to develop until the middle of the 3rd century. After the conquest the border defense system (*limes*) of the new province was established, similar to other parts of the Roman Empire. On the borderline – the outer defensive line of the circular defence system – auxiliary units were stationed [1,2], while in the central part and on the more vulnerable western border the auxiliary units and legions were also positioned. Due to the frequency of barbaric incursions and the economic and political instability of the Empire, the emperor Aurelianus abandoned the province at the beginning of the 270's and withdrew the army to the Danube defence line.

In the line of the *limes* in today's Mureş (Maros) County, we know of three auxiliary forts, along with their adjoining settlements which are located in today's Brâncoveneşti (Marosvécs), Călugăreni (Mikháza) and Sărăţeni (Sóvárad).

The Călugăreni auxiliary fort played an important strategic role in the defence of the Niraj (Nyárád) valley. During the 2nd and 3rd century, the more than forty hectares site was the most important economic and military centre in the region. Based on archaeological prospections and geophysical surveys, the ground plan and the layout of the 2.3-hectare large rectangular fort (*castrum / castellum*) strictly followed the rules of Roman military architecture.

The fort was oriented NE-SW and is located in the central part of the archaeological site. [3, 4] The settlement (*vicus militaris*) developed around it and is located in the western part of the present village and the arable land between Călugăreni and Dămieni (Deményháza). (**Figure 1.** and **2.**)

The main aim of the current excavation is to investigate the headquarter building (*principia*) located at the crossroads of major roads of the fort and a residential area from the *vicus*.

Figure 1. *The excavation areas at the (1) vicus and the (2) auxiliary fort (made by Nándor Laczkó)*

Figure 2. *Virtual reconstruction of the site (made by Zsolt Vasáros)*

2. Experimental

2.1. Brief review of the samples

The iron slag samples studied are presented in **Table 1.** Most of them were unearthed at the residential area discovered at the Călugăreni military settlement (vicus) during the excavations performed in 2013–2014, situated on the trench C, C1, C2 of the site. The finds discovered after 2015 belong to the trenches A2, A5, A2015 and A6 from the 3rd century phase of the headquarter building (principia). In the selection of the samples chosen for this study, besides the archaeological relevance, the assurance of the adequate probe quantity in order to complete the planned investigations was considered.

Macroscopic characterization of the samples was performed by visual examination, in daylight, under a magnifying glass of 5x magnifying power. The macrophotos were obtained using a LUMIX TS7 digital camera of 20.4 Megapixels, at the same time and in the same conditions, and are presented in **Figure 3.** and **4.**

Due to the relatively small number of specimens selected, the classification of the probes associated with the excavation trench and the context and macroscopic characteristics was not possible.

The samples collected on the vicus territory typically are partially glassy, with dark grey and/or black zones on the outer surfaces, containing various quantity of differently sized gas inclusions (lunkers, vesicles) and iron inclusions (metallic droplets).

The macroscopic morphology of the samples 2008, 2155, 2355, 2356, 4009 and 4264 is pumiceous (spongy) and pronouncedly vesicular (with many gas lunkers) assuring their low density. They are very heterogeneous, with greyish, reddish, blackish, clayish-yellow with more or less crystallized or glassy zones on the surface. In

Table 1. *The iron slag samples*

No.	Small find no.	Trench	Context	Excav. year
Finds from the *vicus*				
1	2008	C	2000	2013
2	2155	C	2001	2013
3	2318	C	2005	2013
4	2342	C	2005	2013
5	2355	C	2009	2013
6	2356	C	2009	2013
7	4009	C2	2039	2014
8	4137	C1	2034	2014
9	4169	C2	2039	2014
10	4222	C1	2038	2014
11	4251	C1	2035	2014
12	4264	C1	2038	2014
Finds from the *principia*				
13	10218	A2	109	2015
14	10532	A5	250	2016
15	10661	A5	339	2016
16	10673	A2016	346	2016
17	11145	A6	443	2017

most samples variously sized black magnetite crystals are embedded, and every sample contains – in various quantities – differently sized iron droplets. The inside of the vesicles is usually a blackish, frequently glassy "nest" with metal globules.

The surface of samples 2318, 2340, 4169, 4222 and 4251 is also heterogeneous, but (excepting 2318 with a clayish core) are dark grey or blackish inside. The structure is denser, assuring a greater hardness, so pulverisation is usually difficult. Sample 4137 is sandwich-structured: a 3-4 mm thick terracotta outer layer which covers a 3-4 mm thick black inner layer, which in turn covers a terracotta core.

Macroscopic morphology of the samples unearthed at the principia show some differences when compared to the vicus samples. The relatively dense, stratified 10218 contains plenty of small vesicles. The outer clayish layer is pulverulent, the vitrified core being blackish, with many small metallic globules; so its fracturation and trituration is difficult. The dark grey sample 10532 is compact, with large glassy vesicles nesting
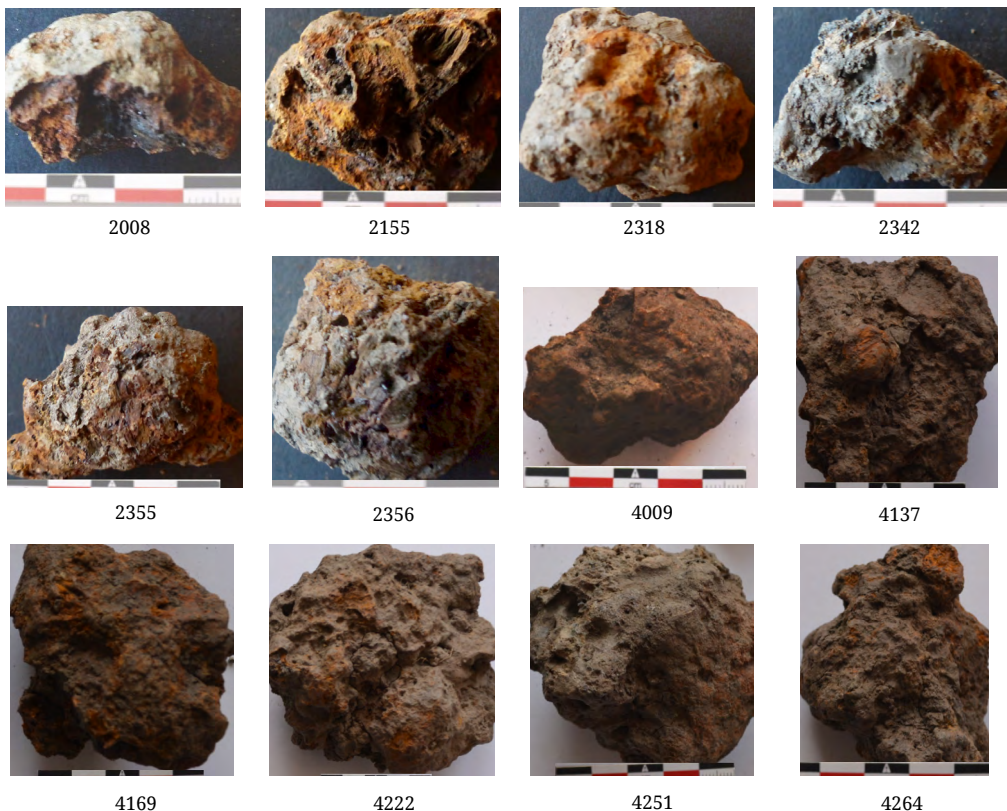

| 2008 | 2155 | 2318 | 2342 |

| 2355 | 2356 | 4009 | 4137 |

| 4169 | 4222 | 4251 | 4264 |

Figure 3. *Macrophotos of the samples finds from the vicus*

| 10218 | 10532 | 10661 | 10673 | 11145 |

Figure 4. *Macrophotos of the samples finds from the principia*

many iron "beads". It is brittle, but its grinding is difficult. The compact 10661 is even harder, but is fissile (easily splits into layers). The surface is grey, the inside is clayish red and with some small iron globules in the blackish cracks. The lighter, spongy, moderately blistered 10673 and 11145 are susceptible to lamellary-columnal fracturation and can be easily ground. Their surface is greyish-red, their core is reddish-clay, lamellar structured, with some white crystalline material, larger magnetite crystals and iron inclusions.

2.2. Investigation methods and results

2.2.1. Optical microscopy (OM)

The microphotos [5, 6] were obtained at 500x magnification on the raw outer surface, and the fresh, rough (unpolished) core surface (cleavage) obtained by crushing the samples, were registered using a Dino-Lite Edge AM4115T digital microscope without polarisation and the DinoCapture 2.0 image processing software. Some of the most characteristic microphotos are presented on the **Figures 5.** és **6.**

The mineralogical interpretation of the OM data obtained (the identification of the mineral components) is in progress, however, some general characteristics of the samples can be concluded.

The totality of the samples contain, in different quantities, differently sized gas lunkers and iron inclusions (metallic droplets separated typically in the inside of the gas holes or in the cracks where they were formed). Additionally, cubic magnetite crystal inclusions appear in every sample, although they are fewer. [7]

2.2.2. FTIR spectroscopy

FTIR spectra of the archaeological finds can be used as a convenient tool for the elucidation of the chemical processes that occured during their genesis (fabrication or simply formation as in the case of the iron slags), and the geochemical (alteration) processes taking place during their burial [8–10]. In the case of the archaeological iron slags, the wide, tipycally medium intensity absorption bands appearing in the 3700-3000 cm^{-1} spectral region, generated by free and (physically or chemically) bonded OH, together with the
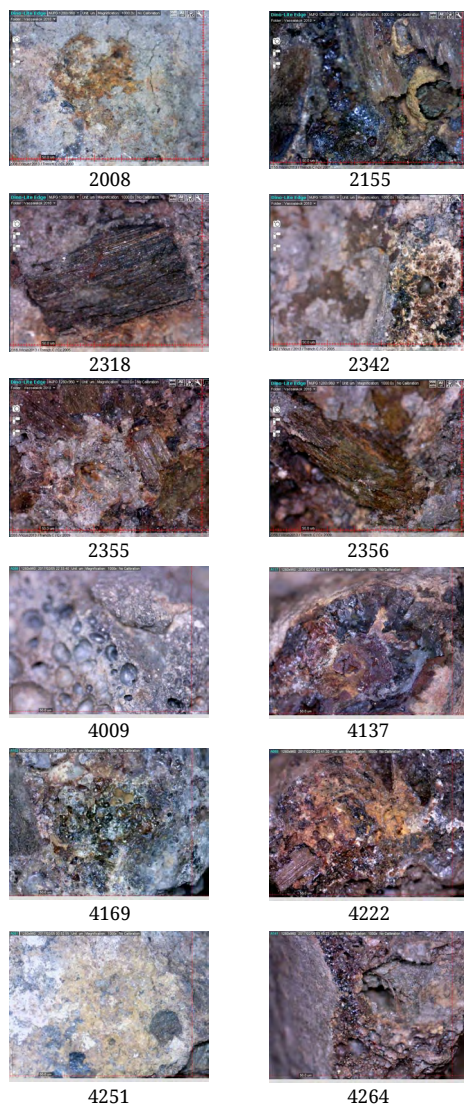

| 2008 | 2155 |

| 2318 | 2342 |

| 2355 | 2356 |

| 4009 | 4137 |

| 4169 | 4222 |

| 4251 | 4264 |

Figure 5. *Selected microphotos of the vicus samples (500x)*
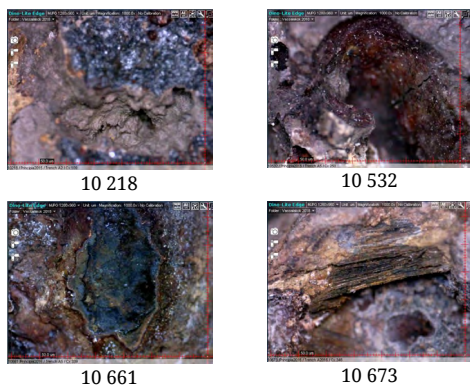
Figure 6. *Microphotos obtained on principia samples (500x)*

Figure 7. *FTIR spectrum of the iron slag surface layer (black) vs. the inside material (red); sample 4009*

wide, intense, quasi-symmetrical (alumino)silicate bands shown between 1100-1000 cm⁻¹, reliably characterize the structural order (or disorder) of the samples. Structural ordering of the iron slags is the result of the crystallization that occurred during the cooling of the melted material, followed by the metamorphosis (alteration) processes occurring during burial, the latter largely depending on the local environmental particularities of the archaeological site. The spectral components identified by means of the spectral deconvolution of the above mentioned main absorpion bands can confirm (reinforce) the mineralogical componency resulting from the petrographic microscopy, XRD and macroelemental analysis data of the samples.

The FTIR absorption spectra in the 4000-400 cm⁻¹ region were obtained on KBr pellets of the agate mortar pulverised samples witho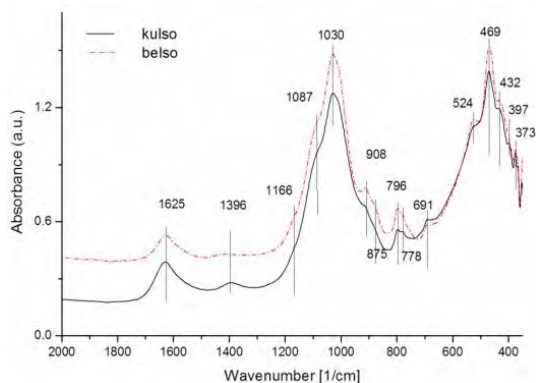ut any kind of prior thermal treatment. The spectra were re-corded using a JASCO FTIR 6100 spectrometer of 1 cm⁻¹ resolution. The composition of the pulverised samples was, as far as possible, close to the homogenized bulk composition. FTIR spectra on the surface layer and the inside of the 4009 sample in the 2000-400. cm⁻¹ region were also recorded (**Figure 7.**)

Due to the absence of deconvolution data in relation to the major OH absorption band, an adequate interpretation of the 4000-2000 cm⁻¹ spectral region is uncertain, assignation of the main absorption peaks was made in the 2000-400 cm⁻¹ region (**Table 2.** presents the data obtained for the vicus samples 4009-4264).

As an exception, in case of three selected samples that presented a peculiar archaeological interest (the 2155, from the vicus, and the 10218 and 10532, from the principia), the peak assignation was extended to the whole spectrum (**Figure 8.**, **Table 3.**).

**Table 2.** *Assignments of the FTIR absorption peaks (bulk) in the 2000-400 cm⁻¹ region*

Wavenumbers (cm⁻¹)						Assignments*
4009	**4137**	**4169**	**4222**	**4251**	**4264**	
1630	1620	1625	1620	1627	1630	OH, FeO(OH)
1394 sh	1698	1396	1396	1394	1401	CO_2
1167 sh 1076 sh 1045	1084 sh 1029	1166 sh 1087 sh 1030	1166 sh 1087 sh 1030	1094 sh 1025	1165 sh 1080 sh 1023	SiO_4, AlO_4 dominant mode FeO(OH) 1084
913 876	882	908 875	908 875	906 sh	913 sh	Fe_2O_3 1100 CO_2 880-860
794 776	796 779	796 778	796 778	798	796 778	SiO_4, AlO_4 dominant mode FeO(OH) 803
524 462 421	526 467 435	524 469 462 sh	524 469 462 sh	524 sh 467 428	526 sh 471 421	Fe_2O_3 550, 417 FeO(OH) 470, 410 Si-O, Al-O, 470-460

* Based on the RRUFF database
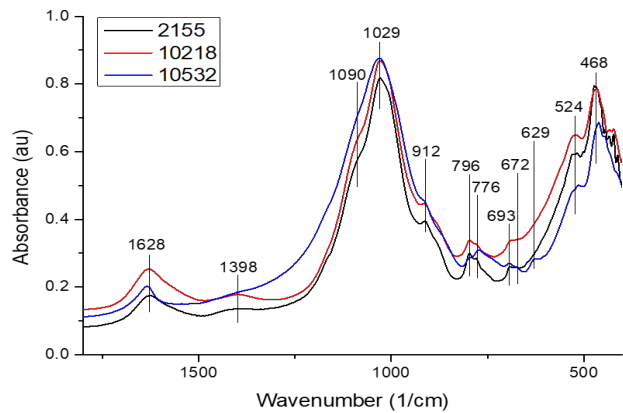
a.
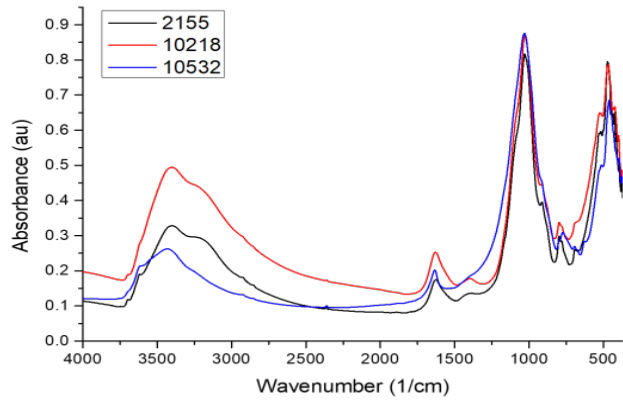
b.
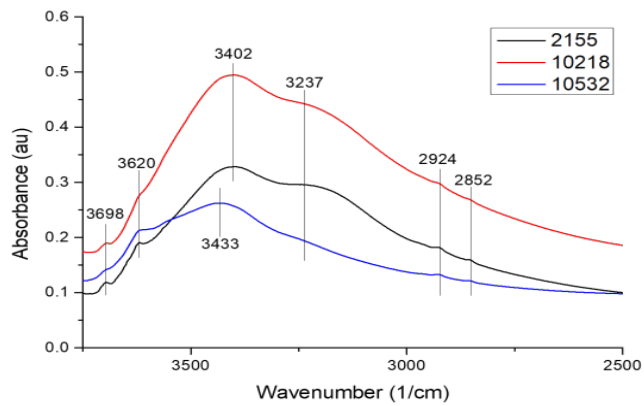
c.

Figure 8. *FTIR spectra of three iron slags selected for detailed characterization:*
(a) 4000–400 cm^{-1}, (b) 4000–2500 cm^{-1}, (c) 2000–400 cm^{-1}

Table 3. *FTIR data of the three selected samples in the 4000-400 cm^{-1} region*

Wavenumbers (cm^{-1})			Assignments*
2155	10218	10532	
3618	3621	3616	OH
		3549	
3401	3403		
3221	3220	3243	
2923	2924	2914	
2853	2851	2854	
1627	1629	1635	
1398	1398	1393	SiO$_4$
1090	1090		SiO$_4$, AlO$_4$ 1100-900 FeO(OH), Fe$_2$O$_3$ 1105, 1084
1029	1030	1030	
912	915	914	
797	797	799	SiO$_4$ 798-782, FeO(OH) 803
779	777	773	FeO(OH)
693	695	693	AlO$_4$
		627	SiO$_4$ 630
520	523	515	Fe$_2$O$_3$
471	465	431	FeO(OH) 470 Fe$_2$O$_3$ 432

According to **Figure 7.**, in the case of sample 4009, the FTIR spectra corresponding to the outer layer and the inside of the sample in the 2000-400 cm^{-1} region practically coincide. This indicates that even if some geochemical processes took place during burial, their influence, at least in this case, is negligible. Corroborating this with the **Table 2.** data (which indicate a parallelism of the spectral behaviour of the different samples), it is probable that in most cases the FTIR study carried out on probes corresponding to the bulky composition of the samples is good enough.

Comparing the absorption peak assignments presented in the **Table 2.** and **3.** indicates that the FTIR spectroscopic behaviour of the two sample groups (from the vicus and the principia), at least in the region 2000-400 cm^{-1}, is also similar, even if some minor differences can be observed. So far, in case of the Călugăreni site, the FTIR spectroscopic behaviour of the slag samples does not depend on the exact location where they were unearthed. However, this conclusion (or further conclusions) needs more data obtained by further methods, such as the actual ongoing XRD, XRF, ICPMS investigations.

3. Conclusions

The Roman auxiliary fort located at Călugăreni, on the Eastern sector of the Dacian *limes*, established after the Roman conquest of the Dacian kingdom, was a strategically important military centre. During the still ongoing archaeological excavations a large quantity of iron slag remains have been unearthed. However, to date, no trace of bloomery or smithery workshops was found at the location. In consequence, the source of the slag finds is unknown; they could originate equally from the local processing of some imported iron blooms, or from the recovery of damaged iron objects (weapons and household tools) by reparation or recycling. The issue could be clarified to some extent by means of the archaeometric study of the slag finds. In this case, the thorough investigation of 17 carefully selected iron slag samples was initiated. In this first stage, after a macroscopic evaluation of the morphology, optical microscopy and FTIR spectroscopy was carried out on the specimens.

According to the characteristic FTIR absorption peaks appearing in the spectral domain 2000-400 cm^{-1}, the investigated samples among some carbonates (and possibly aluminates) are constituted from silicates. The carbonates could have been formed in carbonation processes taking place during burial, as a consequence of the environmental conditions.

According to the microphotos registered, the main crystal phase of the samples identified in the absence of polarized light is fayalite (Fe$_2$SiO$_4$); dendritic wüstite and cubic magnetite are also observed in practically every sample. The samples generally are characterized by a vast amount of metallic iron inclusions, and the presence of some glassy phases. These considerations indicate that the (smelting or smithy) processes the samples were subjected to took place at relatively high temperatures, probably in a reducing atmosphere or environment.

According to the macroscopic characteristics, the possibility that the slags could be smelting by-products can't be excluded. The morphology of some samples are close to that of the tap slags: these specimens are more dense, with small blow holes inside, as the tap slag froze outside the smelter. The lower density, sponge-like structured samples full of gas lunkers seem to have been cooled down inside the smelter (cinder).

In future, research will continue with petrographic microscopic and XRD investigation, and

macro- and microelemental analysis of the samples. Naturally, we have to keep in mind that (as indicated by the standard deviation values associated with the previous PXRF elemental analyses of the surface composition of similar samples) these types of sample are very heterogeneous. **[11, 12]**. In consequence, conclusions referring to the slag's mineralogical and/or chemical composition have to be drawn very cautiously.

Acknowledgement

References

[1] Matei-Popescu F., Ţentea O.: *The Eastern Frontier of Dacia. A Gazetteer of the Forts and Units.* In: Orbis Romanus and Barbaricum. The Barbarians around the Province of Dacia and Their Relations with the Roman Empire. (Ed.: Bârcă V.). Mega Publishing House, Cluj-Napoca, 2016. 7–24.

[2] Höpken C. et al.: *Wachtürme am Dakischen Ostlimes zwischen Brâncoveneşti und Călugăreni (jud. Mureş/RO).* Archäologisches Korrespondenzblatt 46. (2016) 241–254.

[3] Pánczél Sz. P.: *The Roman Fort from Călugăreni (Mureş County, Romania).* In: LIMES XXII. Procee-
dings of the 22nd International Congress of Roman Frontier Studies Ruse, Bulgaria, September 2012. (Eds.: Vagalinski L., Sharankov N.). National Archaeological Institute with Museum, Sofia, 2015. 909–916.

[4] Pánczél Sz. P. et al.: *A mikházi római segédcsapattábor kutatása/The research at the Roman auxiliary fort of Mikháza/Călugăreni.* Magyar Régészet/ Hungarian Archaeology, 2018 spring, 13–20.
http://files.archaeolingua.hu/2018TA/Pa%b4ncze%b4l_E18TA.pdf

[5] Buchwald V. F., Wivel H.: *Slag analysis as a method for the characterization and provenancing of ancient iron objects.* Materials Characterization, 40. (1998) 73–96.
https://doi.org/10.1016/S1044-5803(97)00105-8

[6] Kramar S. et al.: *Mineralogical and geochemical characterization of Roman slag from the archaeological site near Mosnje (Slovenia).* Materials and technology, 49. (2015) 343–348.
http://mit.imt.si/Revija/izvodi/mit153/kramar.pdf

[7] Mihailova I., Mehandjiev D.: *Characterization of fayalite from copper slags.* Journal of the University of Chemical Technology and Metallurgy 45. (2010) 317–326.
http://dl.uctm.edu/journal/node/j2010-3/12_Irena_Mihailova_317-326.pdf

[8] Sowmya T., Sankaranarayanan S. R.: *Spectroscopic analysis of slags – preliminary observations.* In: VII. International Conference on Molten Slags, Fluxes and Salts, The South African Institute of Mining and Metallurgy, South Africa, 2004. 693–697.
http://www.saimm.co.za/Conferences/MoltenSlags2004/693-Sowmya.pdf

[9] Olovčić A., Memić M, Žero S, Huremović J., Kahrović E.: *Chemical Analysis of Iron Slags and Metallic Artefacts from Early Iron Age.* International Research Journal of Pure and Applied Chemistry, 4. (2014) 859–870.
https://doi.org/10.9734/IRJPAC/2014/12248

[10] Sheikh M. R. et al.: *Characterization of iron slag of Kakching, Manipur by X-ray and optical spectroscopy.* Indian Journal of Pure & Applied Physic, 48. (2010) 632–634.
http://nopr.niscair.res.in/bitstream/123456789/10153/1/IJPAP%2048%289%29%20632-634.pdf

[11] Chuenpee T., Won-In K., Natapintu S. Takashima I.: *Archaeometallurgical Studies of Ancient Iron Smelting Slags from Ban Khao Din Tai Archaeological Site, Northeastern Thailand.* Journal of Applied Sciences, 14. (2014) 938–943.
https://doi.org/10.3923/jas.2014.938.943

[12] Scott R. B. Eekelers K., Degryse P.: *Quantitative chemical analysis of archaeological slag material using handheld X-ray fluorescence spectrometry.* Applied spectroscopy, 70. (2016) 94–109.
https://doi.org/10.1177/0003702815616741